Int. J. Rock Mech. Min. Sci. & Geomech. Abstr. Vol. 13, pp. 155–163. Pergamon Press 1976. Printed in Great Britain

The Role of Asperity Indentation and Ploughing in Rock Friction—II.

Influence of Relative Hardness and Normal Load

J. T. ENGELDER*
C. H. SCHOLZ†

The frictional characteristics of rock forming minerals depend on the relative hardness of the asperity and substrate (flat) upon which it slides; an asperity with a scratch hardness less than a polished flat has a lower static coefficient of friction (μ_s) on that flat than an asperity with a scratch hardness greater than the same flat. Frictional wear associated with the slip of asperities consists of: (1) ploughing by plastic deformation; (2) ploughing by brittle fracture; (3) fracture of the asperity. Stick–slip correlates with ploughing by brittle fracture. Using Griffith's criteria for propagation of flaws, Hertz's analysis for ring cracking and Hamilton and Goodman's analysis for partial ring cracking under an asperity the normal load necessary for crack propagation and thus the onset of stick–slip may be predicted. The propagation of cracks during ploughing by brittle fracture is one mechanism of time-dependent friction.

INTRODUCTION

In the classical theory of friction the origin of frictional forces are traced to components of adhesion, ploughing and roughness. The first component is the force necessary to shear junctions where two sliding surfaces have adhered to one another. The second is the force necessary to move a hard asperity while it ploughs a groove into a relatively softer substrate. The third is the force necessary to slide one surface up over roughnesses on the opposite surface.

Recent interest in the frictional characteristics of rocks has precipitated questions about the suitability of the classical theory for describing the origin of frictional forces between rocks. In the companion paper [pp. 149–159] we established that Bowden and Tabor's [1] adhesion theory, when modified to include asperity creep, adequately accounts for rock friction. Here we will establish the influence of the relative hardnesses of rock forming minerals on the frictional components of ploughing and adhesion. Of particular interest is the role of brittle fracture as a mechanism of asperity creep during adhesion and ploughing.

Previous work

Our investigation of the influence of mineral hardness on ploughing and adhesion is similar to Tabor's [2] in which a metal point (asperity) of intermediate hardness was dragged over a metal strip (Fig. 1). Tabor suitably heat-treated the strip so that one end was rendered soft and the other end hard, with a uniform increase in hardness from end to end. Over the soft portion of the metal the friction was high, the motion was intermittent, and surface damage occurred. The behavior remained much the same until a critical hardness was reached. At the critical hardness the friction dropped and little surface damage was observed. There was a critical difference in scratch hardness between an asperity and flat before scratching of the flat occurred, otherwise the asperity deformed rather than the flat. Tabor [2] showed that an asperity will scratch a flat if it has a hardness 1.2 times that of the flat (Fig. 1).

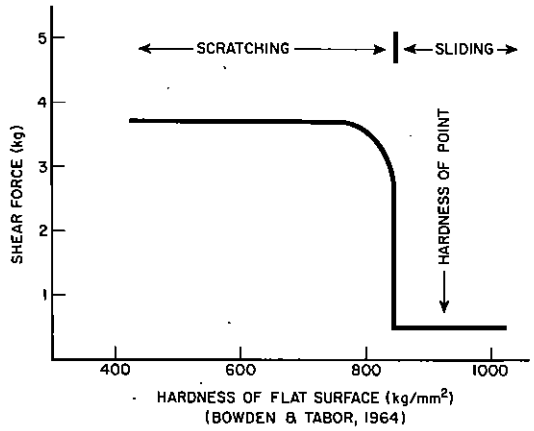

Fig. 1. Friction between a metal point and a metal sheet of varying hardness.

* Lamont-Doherty Geological Observatory of Columbia University, Palisades, NY 10964, U.S.A.
† Lamont-Doherty Geological Observatory of Columbia University, Palisades, NY 10964, U.S.A. Also, at the Dept. of Geological Sciences, Columbia University.

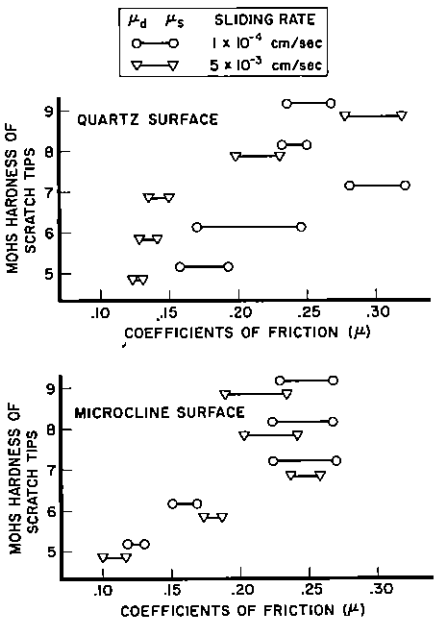

Fig. 4. Friction between various scratch tips and polished surfaces of quartz and microcline.

are those that leave a perceptible scratch in the surface of quartz. Slip without cutting major scratches in the surface of quartz occurs with a much lower μ_s.

The same effect of asperity hardness is seen for slip on microcline except that quartz asperities leave a scratch on microcline and thus have a μ_s equivalent to that of topaz and corundum. We suggest that a slight hardness contrast between orthoclase and microcline causes the difference in friction between quartz on quartz and orthoclase on microcline.

The effect of velocity on μ_s for various points is consistent with a time-dependent friction law. With the exception of corundum on quartz and orthoclase on microcline, the slower displacement rate resulted in a higher μ_s. The most exaggerated effect of velocity is seen for orthoclase and quartz sliding on quartz. A quantitative notion of the effect of velocity was obtained by sliding a diamond asperity on fused silica (Fig. 5). These results verify the logarithmic dependence of friction on time of contact as predicted in the companion paper.

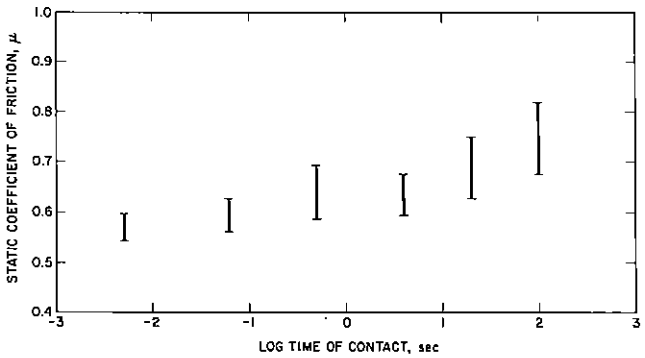

Fig. 5. Variation in μ_s with time of contact for a diamond asperity sliding on fused silica. Time of contact is directly proportional to the sliding rate which was varied between 10 cm/sec and 2×10^{-3} cm/sec.

Frictional wear

Three types of wear tracks observed on the surface of polished quartz are: (1) the track of positive relief caused by an asperity softer than the flat rubbing off on the flat (Fig. 6a); (2) a track of fractures resulting from an asperity passing over a flat of equal hardness (Fig. 6b); and (3) a groove of negative relief caused by an asperity harder than the flat ploughing into the flat (Fig. 6c). An orthoclase asperity sliding on quartz leaves periodic streaks on the quartz surface (Fig. 6a). Wider patches of orthoclase correspond with locations where the asperity was in stationary contact with the flat and sheared off during stick–slip. Careful examination reveals fractures in the quartz radiating from the wear track. The fractures usually form at a high angle to the direction of slip. Quartz asperities sliding on quartz flats result in wear tracks consisting of fractures in the quartz flat at high angles to the direction of slip (Fig. 6b). At higher sliding rates the track of fractures is continuous in contrast to grouped sets of

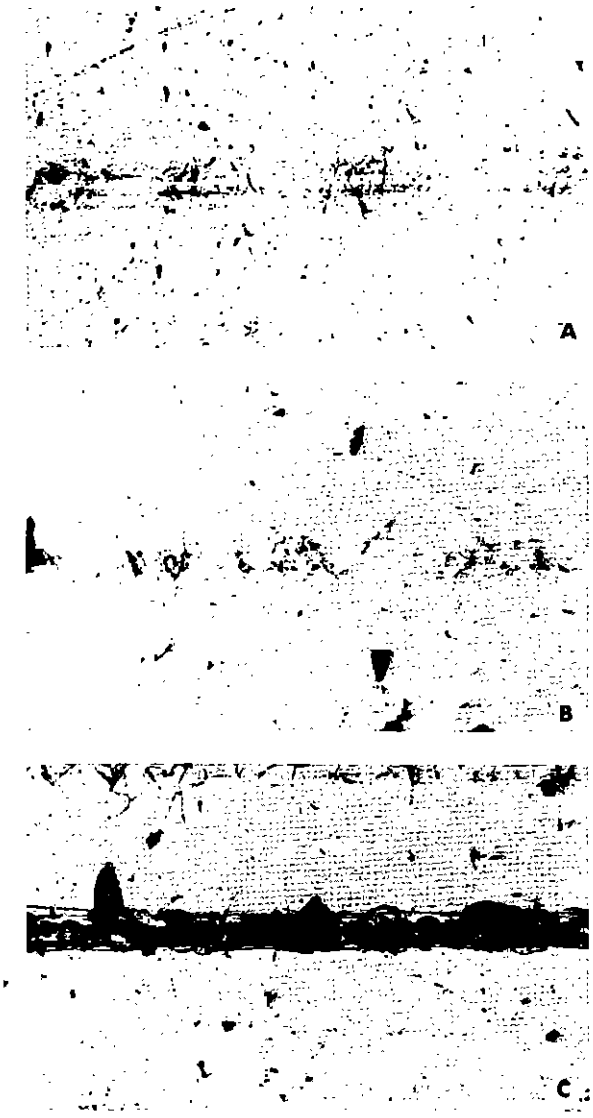

Fig. 6. Wear tracks on the surface of polished quartz. Mineralogy of asperity causing the track: (a) orthoclase; (b) quartz; and (c) corundum. The width of the field of view is 0.022 cm. Asperity moved from left to right.

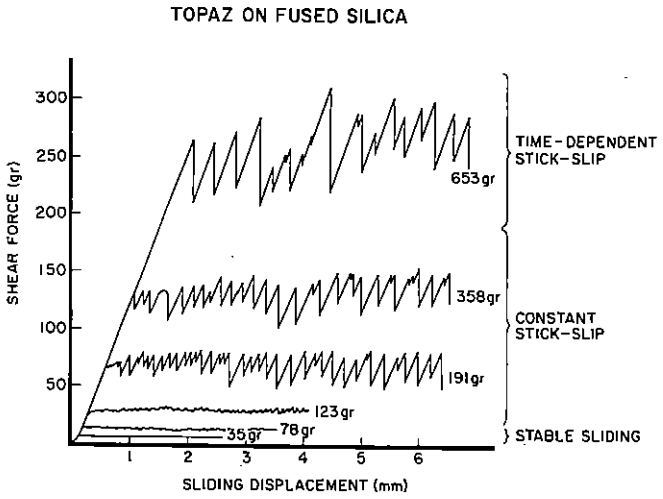

Fig. 8. Shear force vs displacement curves for topaz sliding on fused silica with various normal loads at 5×10^{-3} cm/sec. The sliding modes are labeled.

of magnitude decrease in slip rate for time-dependent stick–slip. In contrast, the change in μ_s with order of magnitude change in slip rate is barely perceptible (<0.01) for constant stick–slip.

These three modes of sliding leave distinct wear tracks on the surface of fused silica. At normal loads of 35 and 78 g the stable sliding of topaz leaves one or more continuous lines on the polished surface. The lines may be resolved only when viewed with high power (200 ×) of a reflecting light microscope (Fig. 9a). The lines are 1–5 μm wide and are small grooves in the surface assumed to be caused by sharp irregularities on the surface of the asperity. Stable sliding is indicated by the continuous nature of the lines as well as the shear force versus displacement plots (Fig. 8).

At normal loads of 123, 191 and 358 g partial ring cracks form during the slip phase of stick–slip sliding (Fig. 9b). The concave side of the partial ring cracks faces the direction of the slip of the asperity on the flat. The partial ring cracks generally form during the first part of each slip event so that a number of partial ring cracks line up in regular intervals in the surface which correspond to the distance slipped during stick–slip. The number of partial ring cracks per slip event increases with normal load.

For normal loads of 653 g or greater partial ring cracks are observed for the entire length of all slip events during stick–slip (Fig. 9c). In addition complete ring cracks may be observed at spots where the asperity was in stationary contact with the polished flat. For normal loads under which complete ring cracks grew the static friction increased with time of contact. This marked time-dependent effect was not observed for experiments in which complete ring cracks did not grow during static contact. Constant stick–slip correlated with those experiments during which ring cracks did not propagate during static contact whereas time-dependent stick–slip correlated with the growth of ring cracks during static contact.

Another correlation is that between brittle fracture and stick–slip. The onset of stick–slip is accompanied by the propagation of fractures into the fused silica. Stable sliding at low normal loads occurred without fracturing the fused silica.

Sapphire

Polished sapphire discs were used to test the effect of normal load on surfaces with a high scratch hardness. None of the five asperities discussed previously were hard enough to scratch sapphire at 358 g normal load where all asperities slide stably at about $\mu_d = 0.15$. The frictional nature of stable sliding on sapphire at $\mu_d = 0.15$ appeared to be the same as stable sliding of topaz on fused silica at normal loads below the stable sliding to stick–slip transition. In both cases friction appeared to arise from adhesion between the point and flat with brittle fracture occurring in the flat.

The corundum scratch tip slid stably on the sapphire flat unless loaded with at least 638 g. Under 638 g normal load partial ring cracks formed and stick–slip sliding occurred. Here the high normal stress necessary

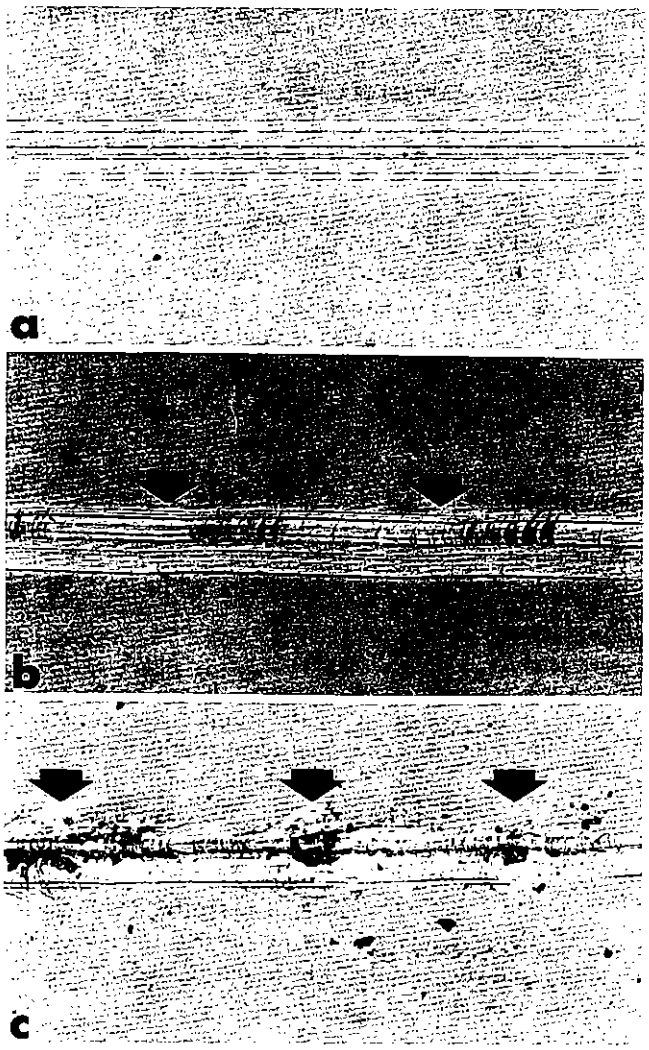

Fig. 9. Wear tracks of topaz asperities sliding on fused silica at three normal loads: (a) 78 g, stable sliding; (b) 191 g, constant stick–slip; and (c) 653 g time-dependent stick–slip. Arrows indicate spots where the topaz asperity was in static contact with the fused silica during stick–slip. Width of field of view is 0.02 cm. Asperity moved from left to right.

(as by the driving in of a wedge). The Griffith fracture analysis corresponds to the first case where a crack of a critical length will grow without limit whereas a shorter crack will not grow. Frank and Lawn suggest that crack growth is initiated at surface flaws which are loaded by a uniform tensile stress. Once crack propagation is initiated the inhomogenous stress field around a spherical indenter results in a loading situation much like the wedge.

In our analysis of frictional sliding we are only interested in conditions necessary for the initiation of fracturing and not in the path a crack takes once it starts to propagate. Therefore we consider only the first part of Frank and Lawn's analysis in which Griffith theory is used. Here the tensile stress σ_G at which a crack or surface flaw of length C will begin to grow in plane strain is:

$$\sigma_G = [2\alpha E/\pi(1 - \nu^2)C]^{1/2}, \tag{7}$$

where α is the surface energy of fracture. If we equate σ_G with σ_m we may calculate the normal load P necessary to initiate crack propagation of surface flaws with a spherical indenter of a certain radius:

$$N = \left[\frac{8\pi\alpha E a^4}{(1 - \nu^2)(1 - 2\nu)^2 C}\right]^{1/2}. \tag{8}$$

The larger the surface flaw the smaller the normal load necessary to initiate fracture propagation.

When a spherical indenter slides on the surface of a brittle solid the inhomogeneous stress field under the indenter is modified from that during static contact. Lawn [12] showed that the maximum tensile stress occurs on the circle of contact between indenter and flat and at the trailing edge of the sliding indenter. The friction between the indenter and flat generates a shear stress which increases the tensile stress of the trailing edge of the sliding indenter and decreases the tensile stress at the leading edge. In this case the maximum tensile stress σ_m experienced by the brittle flat is greater than for the case for static contact between indenter and flat.

Hamilton and Goodman [13] indicate that σ_m depends on the friction μ in the following manner:

$$\sigma_m = \frac{(1 + 15.5\mu)(\frac{1}{2} - \nu)N}{\pi a^2}. \tag{9}$$

Now the normal load necessary to initiate crack propagation under a sliding indenter is:

$$N = \left[\frac{2\pi\alpha E a^4}{(1 - \nu^2)(\frac{1}{2} - \nu)^2(1 + 15.5\mu)^2 C}\right]^{1/2}. \tag{10}$$

Comparing (8) and (10), we can see that the normal load necessary to form ring cracks during static contact is greater by a factor of $1 + 15.5\,\mu$ than that necessary to produce ring cracks during sliding.

Criteria for stick–slip

Using Griffith's criteria for propagation of flaws, Hertz's analysis for ring cracking and Hamilton and Goodman's analysis for partial ring cracking under an asperity, the normal load necessary for crack propagation and thus stick–slip may be predicted. We proceed by plotting the relation between normal load necessary to cause ring cracking in fused silica and length of surface flaws as expressed by equation 8. This curve is line A–A' (Fig. 10) where E for fused silica is 0.7138×10^{12} dyn/cm^2; ν is 0.14; and an estimate of α comes from Gilman's [14] equation:

$$\alpha = Eb^2/d_0\pi, \tag{11}$$

where b is half the $Si\ -0$ distance in fused silica and d_0 is the distance between potential fracture planes of fused silica. If we assume that $2b = d_0 = 1.6 \times 10^{-8}$ cm where $b = 0.8 \times 10^{-8}$ cm is the half $Si\ -0$ distance in low quartz [15], α is 0.289×10^3 dyn/cm. If α is larger than our estimate, the static curve indicates that the smaller the surface flaws the larger the normal load necessary to initiate ring cracking. Although a is a function of N, this curve is calculated using a constant $a = 2.0 \times 10^{-3}$ cm. This value of a comes from the average width of scratch tracks for normal loads between 35 and 600 g. We observed that ring cracks propagated into fused silica from a topaz point when loaded with more than 400 g. Curve A–A' indicates that the fused silica has surface flaws about 10^{-6} cm long.

Equation (10) (curve B–B' in Fig. 10) indicates that ring cracking will occur at much lower loads on the topaz point if the asperity is sliding on the fused silica. At normal loads of 35 and 78 g μ_d is 0.12. These normal loads plot in C vs N space below the curve B–B' which indicates onset of ring cracking during sliding. For these loads we did not observe ring cracking on the fused silica (Fig. 9a). Sliding of these normal loads is either steady or slightly irregular but sharp stress drops are not observed (Fig. 8). The only surface damage consists of small grooves $< 5 \times 10^{-4}$ cm wide which results from plastic flow around small irregularities of the topaz point.

At a normal load of 123 g small stick–slip events occur. One hundred and twenty three grams is the location in C vs N space where the curve for ring cracking during sliding at $\mu_d = 0.12$ is predicted. We did observe

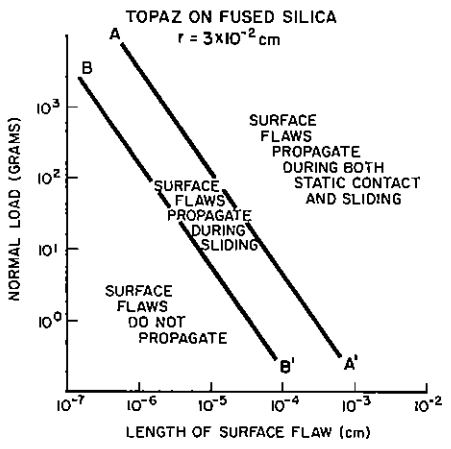

Fig. 10. Normal load necessary for propagation of a certain length surface flaw into fused silica under either a static or sliding spherical topaz indenter of radius $r = 0.002$ cm.

12. Lawn B. R. Partial cone crack formation in a brittle material loaded with a sliding spherical indenter. *Proc. R. Soc.* Part A, **299**, 307–316 (1967).
13. Hamilton G. M. & Goodman L. E. The stress field created by a circular sliding contact. *J. appl. Mech.* **33**, 371–376 (1966).
14. Gilman J. J. Direct measurement of surface energies of crystals. *J. appl. Phys.* **31**, 2208–2218 (1960).
15. Machatschki F. Die Kristallstruktur von Tiefquartz SiO_2 und Aluminiumorthoarsenate $AlAsO_4$. *Zeit. Krist.* **94**, 222–230 (1936).
16. Engelder J. T. Effect of scratch hardness on frictional wear and stick–slip of westerly granite and Cheshire quartzite. In *Proc. NATO Adv. Study Inst. on Petrophysics*, John Wiley, NY, in press (1976).

partial ring cracks on the surface of the fused silica for this load. The static friction increases to more than 0.26 for those tests during which stick–slip occurs. The point on Fig. 10 where $N = 123$ g and $C = 10^{-6}$ cm is on curve B–B' for the onset of ring cracking. The onset of stick–slips correlates with the onset of ring cracking in the fused silica.

For normal loads between 123 g and 358 g partial ring cracking occurs during sliding and not while the surfaces are in stable contact. This observation is confirmed by location of the curve for onset of ring cracking (A–A') for topaz in static contact with fused silica (Fig. 10). Ring cracking occurs during the first part of the slip of a stick–slip cycle. We interpret the intervals without ring cracks as a manifestation of the drop in friction during the stick–slip event. The frictional drop during each stick–slip event has the effect of moving B–B' towards A–A'. This drop in friction has the same effect as dropping the point in C vs N space below B–B'.

Curve A–A' is exceeded for normal loads above 358 g where the entire trace of the scratch track on fused silica contains ring cracks (Fig. 9c). The ring cracks which form under the point in static contact have a circular outline rather than crescent shape. At normal loads greater than 358 g stick–slip is time-dependent; the static friction increases with time of contact. The mechanism of time dependent friction is the same as the mechanism for change with time in Vicker's hardness for olivine and quartz (see companion paper): stress corrosion of cracks. Here the stress corrosion must occur during crack propagation while topaz is in static contact with fused silica. This occurs only if the normal load is large enough to initiate cracking.

In summary, we have stable or irregular sliding at low normal loads where no ring cracking occurs (Fig. 11). Constant stick–slip occurs if the normal load is large enough to initiate cracking during slip but not large enough to cause cracking during stable sliding. Time-dependent stick–slip occurs if the normal load is large enough to cause cracking during static contact. The mechanism of time-dependent stick–slip is stress corrosion of propagating fractures. Engelder [16] showed that stick–slip for polished granite and quartzite occurs above a minimum normal load and that stick–slip correlates with asperity ploughing. Thus for slip of a single asperity as well as a polished rock the normal stress at the stable sliding to stick–slip transition appears to correspond to the normal stress that is sufficient to cause asperity indentation and ploughing.

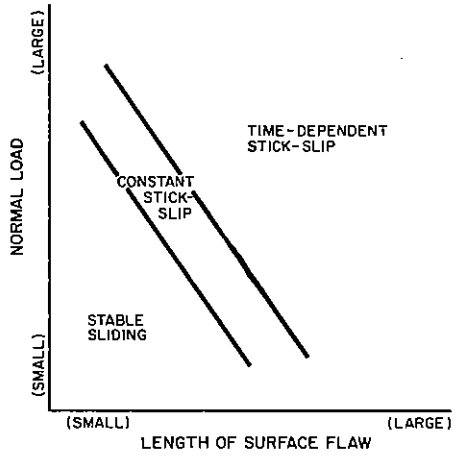

Fig. 11. Schematic of the normal load and surface flaw length criteria for stick–slip. This criteria is based on the correlation between stick–slip and the propagation of brittle fractures.

CONCLUSIONS

We have studied the role of asperity indentation and ploughing in rock friction by observing the friction between asperities and polished surfaces. The effect of scratch hardness on friction may be summed by our observation that asperities with scratch hardnesses less than a polished flat has a lower μ_s on that flat than an asperity with a scratch hardness greater than the same flat. The low friction arises from adhesion between asperity and flat whereas high friction arises from asperity ploughing. We found that stick–slip was commonly associated with the brittle fracture of the flat regardless of the hardness contrast between the asperity and the flat. Finally, asperity indentation creep occurs either by creep of the asperity itself or by penetration of the substrate. Penetration of the substrate by brittle fracture proved to be much more sensitive to time of static contact between asperity and substrate than creep of the asperity.

Acknowledgement—This work was supported by NSF grants GA36357 and GA43295. We thank Lynn Sykes and Paul Richards for critically reviewing the text. Lamont-Doherty Geological Observatory Contribution No. 2339.

Received 5 *November* 1975.

REFERENCES

1. Bowden F. P. & Tabor D. *The Friction and Lubrication of Solids* Vol. 2, p. 544. Clarendon Press, Oxford (1964).
2. Tabor D. Mohs' Hardness scale—a physical interpretation. *Proc. Phys. Soc.* **67**, 249–257 (1954).
3. Rabinowicz E. *Friction and Wear in Materials*, p. 302. John Wiley, NY (1965).
4. Byerlee J. D. Frictional characteristics of granite under high confining pressure. *J. Geophys. Res.* **72**, 3639–3648 (1967).
5. Scholz C., Molnar P. & Johnson T. Detailed studies of frictional sliding of granite and implication for the earthquake mechanism. *J. Geophys. Res.* **77**, 6392–6406 (1972).
6. Brace W. F. Behavior of rock salt, limestone, and anhydrite during indentation. *J. Geophys, Res.* **65**, 1773–1788 (1960).
7. Prandtl L. Uber die Haerte plastischer Koerper. *Goettiger Nachr. math. phys Kl.* 74–85 (1920).
8. Hencky H. Uber eigige statisch bestimate Falle des Gleichgewichts in plastiche Korpern. *Z. angew. Math. Mech.* **3**, 241–250 (1923).
9. Hertz H. On the contact of elastic solids, reprinted in *Miscellaneous Papers*, pp. 146–162. Macmillan, NY (1896).
10. Hertz H. On the contact of rigid elastic solids and on hardness, reprinted in *Miscellaneous Papers*, pp. 163–183. Macmillan, NY (1896).
11. Frank F. C. & Lawn B. R. On the theory of Hertzian fracture. *Proc. R. Soc.* Part A, **299**, 291–306 (1967).

to initiate stick–slip reflects the lack of contrast in hardness between scratch tip and flat. When a diamond asperity was used stick–slip and brittle fracture on polished sapphire occurred at less than 100 g normal load. As was the case for topaz on fused silica, stick–slip correlated with brittle fracture.

Calcite

Solenhofen limestone was used to test the effect of normal load of a polished surface having a very low scratch hardness. Fine grained limestone is used rather than calcite crystals because of the tendency of calcite to cleave. All 5 scratch tips leave a groove resulting from plastic deformation of the polished surface. During ploughing the yield strength of the limestone was exceeded. Sliding occurs on Solenhofen limestone by a combination of stable sliding, episodic sliding and stick–slip. Occasional large stress drops are interspersed among stable sliding and episodic sliding events. Here the frictional characteristics of the asperities on the flat are insensitive to changes in hardness of the scratch tip. All scratch tips are hard enough to plough into the surface in the same manner where $\mu_s = 0.45$.

DISCUSSION

Effect of normal load

We observed three regimes of frictional sliding for a topaz asperity on fused silica: (1) stable sliding; (2) constant stick–slip and (3) time-dependent stick–slip. Each regime corresponded to a different form of frictional wear which was time dependent. At low normal loads the frictional situation is analogous to the experiment in the companion paper [149–154] in which sapphire asperities did not break off and the force (F) required for steady sliding depends on velocity (V) via

$$F = (1 - \beta \log V)\, \mu_d\, N, \tag{1}$$

where N is the normal load and β is a constant. At intermediate normal loads where constant stick–slip occurs, the frictional force necessary to initiate slip is theoretically

$$F = [(1 + \beta \log V) + (1 + \alpha \log t')]\, \mu_d\, N, \tag{2}$$

where t' is time of static contact and α is a constant. The additional time dependent term results from creep of the asperity or flat. Our experience with the topaz asperity on fused silica was that the time-dependent creep of asperity and flat was so small that we could not resolve time-dependent stick–slip from experimental variation over four orders of magnitude change in average sliding velocity. Thus we labeled the stick–slip in which ring cracks did not form during static contact, constant stick–slip.

In contrast, stick–slip which accompanied the formation of ring cracks during static contact was highly time-dependent (Fig. 5). Here the imperceptible creep of the asperity and flat during constant stick–slip was overshadowed by the creep associated with ring crack propagation into the fused silica.

Frictional wear

Our explanation of the frictional behavior of an asperity on a flat surface is based on the competing effects of plastic deformation and brittle fracture. Plastic deformation occurs when the differential stress under the load of the asperity exceeds the yield strength of the flat surface. Brittle fracture occurs when the maximum tensile stress in the flat is large enough to initiate fracture propagation from surface flaws. Depending on the value of such material properties as yield strength, surface energy, and size of surface flaw either plastic deformation, cracking, or both will occur during sliding.

The differential stress under a point load may exceed the plastic yield strength of the crystal under the indentor [6]. Work on indentation by Prandtl [7] and Henchy [8] indicates that two-thirds of the mean pressure during point contact is in the form of hydrostatic pressure. The other third is a differential stress which may be effective in producing plastic flow under the contact point [1]. If plastic flow is to occur under a point load, then

$$N' > 3Y, \tag{3}$$

where N' is the pressure between indenter and indentation and Y is the plastic yield strength of the indented material. At low normal loads irregularities on the topaz asperity cause scratches by plastically deforming the fused silica (Fig. 9a). Friction results from this ploughing.

Once a critical load is exceeded a ring crack (Hertzian fracture) will propagate when a spherical indenter is pressed into a flat surface of a brittle solid. An inhomogenous stress field occurs in the solid under the spherical indenter [9, 10]. From the Hertzian analysis the maximum tensile stress σ_m in the specimen resulting from the load of a spherical indenter is:

$$\sigma_m = (1 - 2\nu)\, N/2\pi a^2 \tag{4}$$

$$a^3 = 4/3\; kNr/E \tag{5}$$

$$k = 9/16[(1 - \nu^2) + (1 - \nu'^2)\, E/E'], \tag{6}$$

where N is the normal load of the indenter, a is the radius of the circle of contact between the spherical indenter and the flat specimen, r is the indenter radius, E and E' are the Young's modulus of specimen and indenter respectively, and ν and ν' the corresponding values of the Poisson ratio [11]. The greatest tensile stress occurs at the edge of the circle of contact between indenter and flat surface. To a first approximation cracking proceeds orthogonally to the greatest tensile stress. The Hertzian fracture starts at the free surface at a point of σ_m. It then propagates around the periphery of the indenter contact and down from the surface in a widening cone.

Frank & Lawn [11] consider the critical conditions for Hertzian fracture and the progress of a crack into the brittle solid. In their analysis they describe the behavior of cracks under two types of simple loading: (1) uniform tensile stress and (2) loading at the mouth

deeper fractures at lower sliding rates. In the latter case the larger shear force drops occur during stick–slip. Topaz and corundum both leave grooves in the surface of quartz and under identical sliding conditions the corundum groove is wider than the topaz groove (Fig. 6c).

Correlation of friction and wear

There are reasonable explanations for several unusual aspects of the data presented in Figs. 3 and 4. One example is the contrast in friction between orthoclase sliding on quartz at 1×10^{-4} cm/sec where μ_s was as high as topaz and corundum vs friction at 5×10^{-3} cm/sec where μ_s was as low as quartz and apatite on quartz. During the longer periods of static contact associated with the slower sliding rate the orthoclase asperity indents into the quartz surface which fractures under the weight of the asperity. The indentation requires a higher shear stress to initiate sliding than would be necessary if the orthoclase were sitting on the quartz without fracturing the surface. Because of the indentation a higher friction develops which approaches that for corundum and topaz sliding on quartz. Once a slip is initiated the orthoclase asperity does not plough but rather slides on the quartz surface. In contrast, the topaz and corundum asperities continue to plough after the onset of sliding. A much higher μ_d results from the process of ploughing during slip than from sliding without ploughing. The large stress drops associated with feldspar asperities relative to topaz and corundum (Fig. 3) are attributed to the low friction accompanying slip without ploughing and consequent high contrast between μ_s and μ_d.

We observed fractures in the quartz or microcline flat under the path of the asperity whenever stick–skip occurred. This was true regardless of the hardness contrast between asperity and flat. For example fractures were observed in quartz over which an apatite asperity had slid. There was a correlation between hardness contrast and fracture spacing. Fractures were periodically spaced in hard flats on which softer asperities had slid. Here the fractures were located under the position of static contact of the asperity. In contrast, fractures were observed for the entire length of slip within flats on which asperities harder than the flats had slid.

A conclusion of the companion paper is that indentation is time-dependent. Time-dependence is demonstrated in Figs. 4 and 5 although for apatite, orthoclase and quartz asperities on quartz flats the effect is larger than expected for a logarithmic dependence. The more rapid increase in μ_s with time is due to the addition of at least two time-dependent effects: (1) indentation into a flat and (2) creep of the asperity. This exaggerated effect is, however, not present for sliding on polished microcline.

μ_s Of corundum, topaz and quartz on the polished microcline is independent of tip hardness. Here friction is controlled by ploughing into the relatively softer flat surface. Asperities with lower scratch hardnesses than surfaces on which they slide have lower coefficients of friction than asperities which are harder than flats and which plough. We conclude that the frictional force associated with adhesion is lower than the force associated with ploughing.

EFFECT OF LOAD ON ASPERITY FRICTION

Many experimentalists have reported that some rocks slide stably at low normal loads but stick–slip at high loads [4, 5]. Assuming that stick–slip is a reasonable mechanism for earthquakes, this change in sliding mode indicates that earthquakes may be restricted to areas within the crust where conditions favor stick–slip. Understanding the effect of normal load on asperity friction is a necessary step toward understanding why certain modes of frictional sliding are favored.

To consider the effect of normal load we slid asperities of topaz, quartz and orthoclase on polished surfaces of fused silica which has a Mohs hardness of 4.9 (Fig. 7). Above a threshold of about 150 g friction of quartz or topaz is much higher than feldspar. This observation is similar to that reported by Bowden and Tabor [1] (Fig. 1) and for our experiments on quartz and microcline flats. When the asperity is about 1.2 times as hard as the flat, friction is higher than for less hard asperities providing time-dependent creep during stick–slip does not increase the friction of a soft asperity on a harder flat. Orthoclase is more than 1.2 times harder than fused silica indicating that the hardness contrast for higher friction is not always 1.2. We also observe that the coefficient of friction increases with normal load up to a certain load above which it becomes constant. The sliding mode as well as friction varies with normal load (Fig. 8). At low loads stable sliding is observed whereas stick–slip occurs at higher loads. Here we identify two categories of stick–slip: (1) constant and (2) time-dependent. The difference between constant and time-dependent stick–slip is the amount that μ_s changes with each incremental change in sliding rate. μ_s Increases as much as 0.05 per order

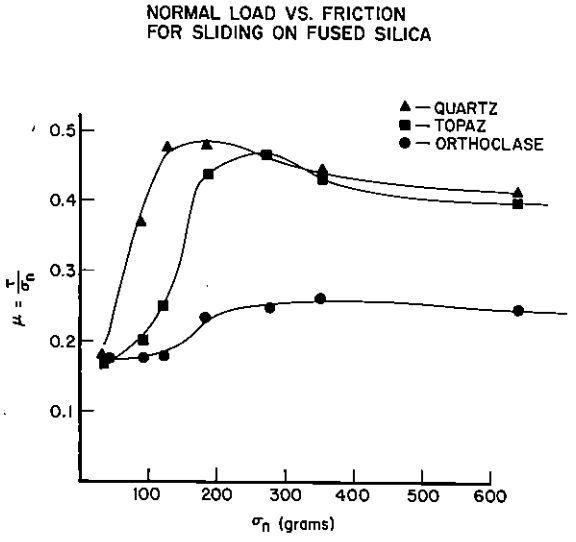

Fig. 7. μ_s Normal load (N) for orthoclase, quartz and topaz asperities sliding on fused silica.

Adhesion and ploughing result in two distinct forms of frictional wear [3]. The deformation of the asperity and the scratching of the flat are manifestations of frictional wear which can be attributed to these two components of friction. In general the deformation of asperities is equivalent to adhesive wear whose fragments are pulled off one surface upon adhering to the other surface. Scratching of the flat is related to abrasive wear where one surface ploughs a series of grooves into the other surface. The relative dominance of these two mechanisms of frictional wear depends to a large degree on the hardness contrast of the minerals in contact at the sliding surface.

We will extend Tabor's work to include geologically common minerals, some of which have a tendency to fracture over the range of pressures and temperatures corresponding to conditions of the upper crust. In the case of rocks brittle fracture modifies notions about friction which have been inferred from experiments with metals.

EXPERIMENTAL PROCEDURE

Our tests consisted of moving a flat surface of a specified hardness under a scratch tip which we shall refer to as an asperity. The flat surfaces included: (1) crystals of quartz and orthoclase with flat surfaces saw-cut and polished with 0.3 μm Linde A polishing compound; (2) flat surfaces of Solenhofen Limestone prepared in the same manner; and (3) polished discs of fused silica and synthetic sapphire (Union Carbide). The asperities, apatite, orthoclase, quartz, topaz, corundum and diamond came from a Ward's Scientific scratch hardness kit. These scratch tips have Mohs hardness of 5, 6, 7, 8, 9, and 10 respectively. The tips with the exception of diamond and corundum were shaped by polishing with emery paper to a hemisphere with a consistent radius of curvature of 3×10^{-2} cm.

The testing apparatus consisted of a cart pulled under an asperity attached to a lever arm which was constrained from flexing in a horizontal direction by a 0.102 cm thick plate of beryllium–copper (Fig. 2). The asperity was loaded by placing the appropriate weight on the lever arm which pivots about a horizontal rod and thus allows the scratch-tip to move freely up and down on the sliding surface. Strain gages bonded to the beryllium–copper plate were used to detect the horizontal deflection of the asperity and thus measure the shear force between the moving flat and asperity. Shear forces may be measured accurately to $\pm$ 250 dyn. A synchronous motor drove the cart through a rack and pinion at a constant rate. The rate of advance was varied between 0.5 cm/sec and 10^{-4} cm/sec by using synchronous motors of various speeds. To minimize vibration from rolling friction, the cart was pulled down way-rods on a set of Thompson ball bearings. Displacement of the cart was measured with a (L.V.D.T.) linear displacement transducer which measures displacements accurately to $\pm$ 0.0001 cm.

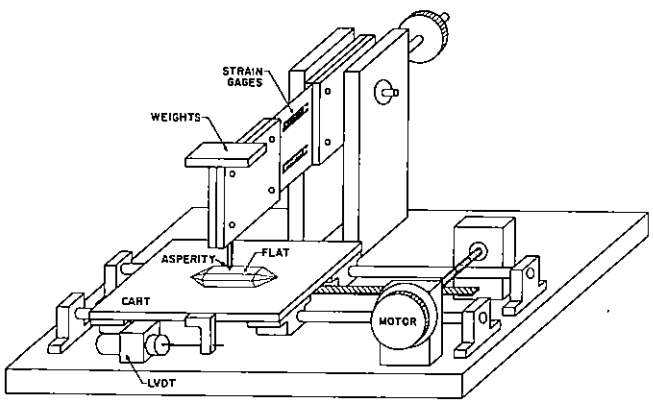

Fig. 2. Test apparatus designed to slide a polished surface (flat) under an asperity.

INFLUENCE OF SCRATCH HARDNESS ON ASPERITY FRICTION

Asperities of apatite, orthoclase, quartz, topaz and corundum were slid on polished quartz and microcline. Asperity load was 358 g in all tests and sliding rates were either 5×10^{-3} cm/sec or 10^{-4} cm/sec. In all cases slip was irregular and in general stick–slip occurred. Examples of the variation of shear force with displacement of the cart are illustrated in Fig. 3. Apatite slid on microcline with relatively low friction and small stress drops whereas corundum slid on quartz with relatively high friction and intermediate stress drops. Orthoclase sliding on quartz at 10^{-4} cm/sec had the largest stress drops observed.

The static coefficient of friction, μ_s, varies with the hardness of the asperity, the hardness of the flat and the rate of displacement of the flat. Consider asperities of five hardnesses sliding on polished quartz at 5×10^{-3} cm/sec (Fig. 4). The hardest asperity, corundum, has the highest μ_s and the softest asperity, apatite, has the lowest μ_s. The two asperities with a high μ_s

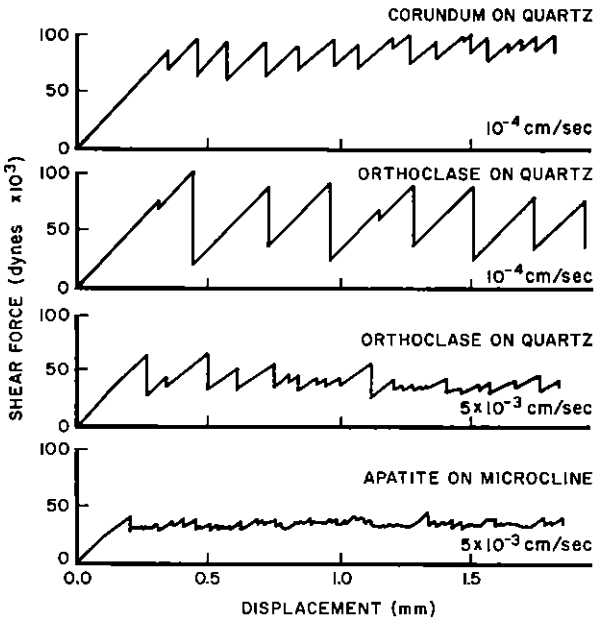

Fig. 3. Shear force vs displacement for sliding of various asperities on polished quartz and microcline.